ELSEVIER

Surface Science 482–485 (2001) 878–885

SURFACE SCIENCE

www.elsevier.nl/locate/susc

STM study of dynamical effects on submonolayer phases of Pb/Si(1 1 1)

O. Custance [a], I. Brihuega [a], J.-Y. Veuillen [b], J.M. Gómez-Rodríguez [a,*], A.M. Baró [a]

[a] *Departamento de Física de la Materia Condensada, C-III, Universidad Autónoma de Madrid, Cantoblanco, E-28049 Madrid, Spain*
[b] *Laboratoire d'Etudes des Propriétés Electroniques des Solides – Centre National de la Recherche Scientifique, B.P. 166, F-38042 Grenoble Cédex 9, France*

Abstract

By means of STM we have been able to analyze in real time the complex dynamical processes that take place at room temperature in the interface between Pb/Si(1 1 1)-(1 × 1) and 1/3 ML α-Pb/Si(1 1 1)-($\sqrt{3} \times \sqrt{3}$)*R*30° reconstructions. We have found that the border between these reconstructions is highly mobile, showing a fluctuating character between 1 × 1 regions and defect free areas presenting the α-($\sqrt{3} \times \sqrt{3}$)*R*30° reconstruction. These fluctuations involve a large number of atoms in cooperative movement as well as atom recombination in the border of the two reconstructions. The intrinsic character of these effects versus possible STM influence has been analyzed and discussed, and a field-induced diffusion mechanism is tentatively suggested.

Keywords: Scanning tunneling microscopy; Epitaxy; Growth; Surface structure, morphology, roughness, and topography; Silicon; Lead

1. Introduction

Pb deposition on Si(1 1 1) surfaces [1–11] can be considered a model system for the analysis of atomic mobility processes with STM. This is mainly due, on one hand, to the relatively low reactive interfaces they form (its mutual bulk solubility is negligible), and, on the other hand, to the adequacy between the rate of atomic motion at room temperature (RT) and typical scanning speeds of STM. In previous works, we have already studied the dynamical processes involved in the first stages of Pb adsorption at RT on Si(1 1 1)-(7 × 7) surfaces [12,13]. In the present work we have focussed our attention on two Pb/Si(1 1 1) phases that can coexist at RT at submonolayer coverage on annealed samples, i.e. Pb/Si(1 1 1)-(1 × 1) and 1/3 ML α-Pb/Si(1 1 1)($\sqrt{3} \times \sqrt{3}$)*R*30° (R3 in the following). By means of STM we have been able to analyze in real time the complex processes that take place at RT in the 1D interface between both reconstructions. Our measurements show that this interface is highly mobile at RT, in accord with a very recent work by Slezák et al.

* Corresponding author. Tel.: +34-91-397-4752; fax: +34-91-397-3961.
E-mail address: josem.gomez@uam.es (J.M. Gómez-Rodríguez).

0039-6028/01/$ - see front matter
PII: S0039-6028(01)00776-2

[14], and displays a fluctuating character between 1×1 regions and defect free areas presenting the R3 reconstruction. The intrinsic character of these effects versus possible STM influence is analyzed and discussed.

2. Experimental

The experiments were carried out in an ultra-high-vacuum (UHV) system composed of two interconnected UHV chambers. The first one contains a home-made beetle-type STM. The second chamber is equipped with low energy electron diffraction (LEED), Auger electron spectroscopy (AES), sample and STM-tip transfer and heating capabilities, several interchangeable evaporation cells, a quartz crystal microbalance and a quadrupole mass spectrometer (QMS). The base pressure of both chambers is below 5×10^{-11} Torr.

Clean reconstructed Si(1 1 1)-7×7 surfaces were prepared by flashing the samples (p-type B-doped Si(1 1 1), resistivity = 0.01 ohm cm) at 1150°C, after carefully degassing at 600°C for several hours. The samples were then slowly cooled down to room temperature (RT). Samples which presented at RT a coexistence of (1×1) and R3 phases were prepared by depositing ~1 monolayer (ML) of Pb on Si(1 1 1)-(7×7) at RT at typical rates of 0.05 ML/min (1ML is defined as the surface atomic density of the Si(1 1 1) surface, i.e. 7.84×10^{14} atoms/cm^2), and subsequent annealing at ~450°C during 4–5 min. Pb was evaporated from a home-built evaporation cell consisting of a Ta boat heated by a filament by electron bombardment. During the evaporation the residual pressure in the UHV chamber remained below 1×10^{-10} Torr and the evaporation rate was monitored by a quartz crystal microbalance and a QMS.

STM data were acquired with a fully automated workstation which incorporates digital feedback control based on DSP (digital signal processor) technology [15]. STM was operated in the constant current mode with variable sample voltages between −2 and +2 V and typical tunnel currents in the range of 0.1 to 1 nA.

3. Results and discussion

STM images of samples prepared by the above mentioned procedure reveal that the surface is composed at RT of regions which present a Pb/Si(1 1 1)-(1×1) reconstruction along with others presenting a R3 reconstruction. The coexistence of these two phases at RT is illustrated in the large scan STM data shown in Fig. 1(a), where the most brilliant areas correspond to (1×1) and the others to R3. It has been reported [4,5] that, for sub-monolayer coverage, two different R3 phases exist

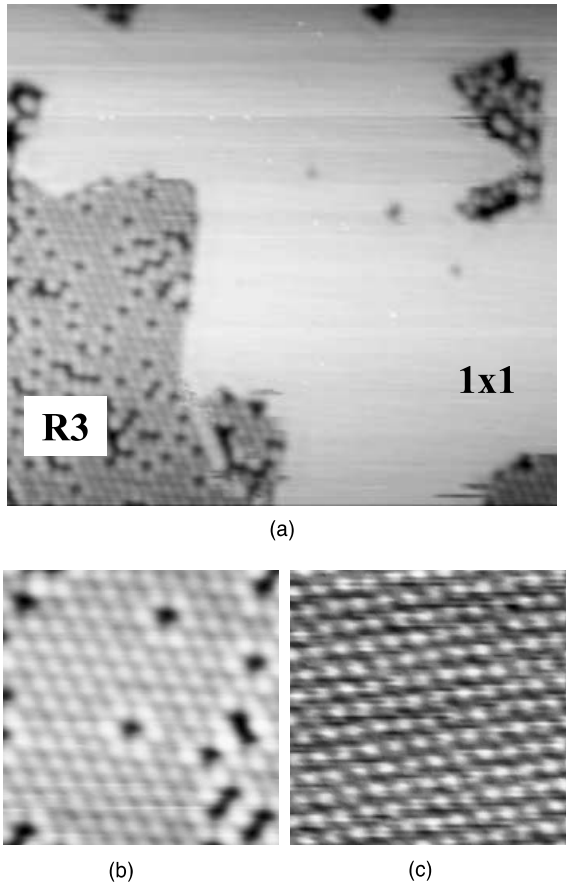

Fig. 1. (a) STM image of Pb/Si(1 1 1) showing the coexistence of (1×1) and R3 phases at RT. The image size is 30×27 nm^2, the sample voltage is −1 V and the tunnel current is 0.2 nA. (b) 8×8 nm^2 atomic resolution STM image of the R3 phase measured at a sample voltage of −1 V and a tunnel current of 0.5 nA. (c) 4.2×4.2 nm^2, atomic resolution image of the (1×1) phase (sample voltage −0.15 V; tunnel current 0.4 nA).

at RT. For a nominal coverage of 1/3 ML, i.e. one Pb atom per unit cell, a R3 pure Pb phase (or α phase) would ideally be found, composed of Pb adatoms sitting on T_4 sites on a bulk terminated Si(1 1 1) surface. For nominal coverages of 1/6 ML it is found a more stable R3 mosaic phase (or γ phase), consisting of a mixture in equal amounts of Pb and Si adatoms [4,5,16] sitting both on T_4 sites. While the mosaic phase can be routinely obtained, the experimental preparation of large domains of pure Pb α-R3 phase is a formidable task. In practice, between 1/3 ML and 1/6 ML local coverage, a pure Pb R3 phase with increasing number of defects (i.e., mainly substitutional Si adatoms, and some vacancies) is obtained. This defective α-R3 phase, which has also been denoted as a solid solution $Si_{1-X}Pb_X$/Si(1 1 1) [17] , is the one that is the object of the present study in relation to the (1×1)-phase. In contrast to the R3 case, the atomic structure of the (1×1)-Pb reconstruction found at RT is not very well known. It has been observed experimentally using several techniques as STM [5], LEED [5] and reflection high energy electron diffraction (RHEED) [19]. STM images display hexagonal arrays of protrusions with the (1×1) periodicity of the Si substrate [5,10,17,18]. It has been proposed that those protrusions correspond to Pb atoms occupying T_1 sites [11], i.e. the local coverage would be one Pb atom per unit cell. In contrast, Seehofer et al. [10] have proposed that the STM (1×1) pattern do not correspond to single Pb atoms but to the result of an averaging process of the highly mobile adsorbates resulting in preferential residence sites. Fig. 1 displays typical atomic resolution images of both phases (R3 in Fig. 1(b) and (1×1) in Fig. 1(c)). For the R3, the difference between lead adatoms and defects (dark in Fig. 1(b)) was realized according to spectroscopic criteria described elsewhere [16].

According to STM images, at RT the boundaries separating (1×1) and R3 domains are rather mobile. An indication of it can already be obtained from careful inspection of the bottom right part of Fig. 1(a), where some strikes can be found in the boundary of the (1×1) region. A systematic investigation of these fluctuations was undertaken by measuring long series of STM movies (i.e. sequential STM images) in the boundaries between (1×1) and R3 domains. The same area spot could be tracked for long times thanks to an STM-drift compensation scheme already described [12]. Fig. 2 shows four frames extracted from one of those STM movies measured on a boundary between a R3 island and a (1×1) region at low sample bias voltage (+0.15 V). Atomic resolution can be visualized in both phases simultaneously. As it can be observed, the small R3 island on the left of Fig. 2(a) enlarges in Fig. 2(b) until it reaches the two defective regions in the right, oscillates in Fig. 2(c) and reduces again to the original size in Fig. 2(d). The changes mainly happen in the R3 defect free area, while the highly defective areas remain almost the same. This fact, observed in most STM movies, suggests that the defects (Si adatoms and vacancies) can act as pinning centers for these fluctuations. Nevertheless, in some cases, the defects found on the boundaries can change its location relative to the R3 layer. This is illustrated in Fig. 3, where some selected frames of another STM movie, measured also at low bias voltage (+0.15 V), are shown. The circles in the figure outline the same spot in the R3 region. As the boundary fluctuates, the disappearance ((b) and (d)) and the change of location (c) of one R3 defect (a) can be observed. This means that fluctuations in the boundaries do not correspond to an overlayer of extra Pb adatoms which grows over the R3 regions, but that a complex rearrangement of the atomic positions of both phases must be accomplished.

A crucial issue that must be addressed is the nature of such complex processes that may involve a large amount of atom displacements at RT. Similar oscillations as those presented here have been reported very recently by Slezák et al. [14] and they were interpreted as the result of thermal fluctuations of the complex 1D interface. STM influence was only detected for temperatures above 210°C when Pb atoms can be desorbed from the surface. No effect was reported, however, for temperatures below this threshold. In the present work, we have undertaken a thorough study of STM influence on such fluctuations. As a first test, STM images were measured on the same areas under different sample bias voltages. Fig. 4 shows the result of one of those measurements. The same

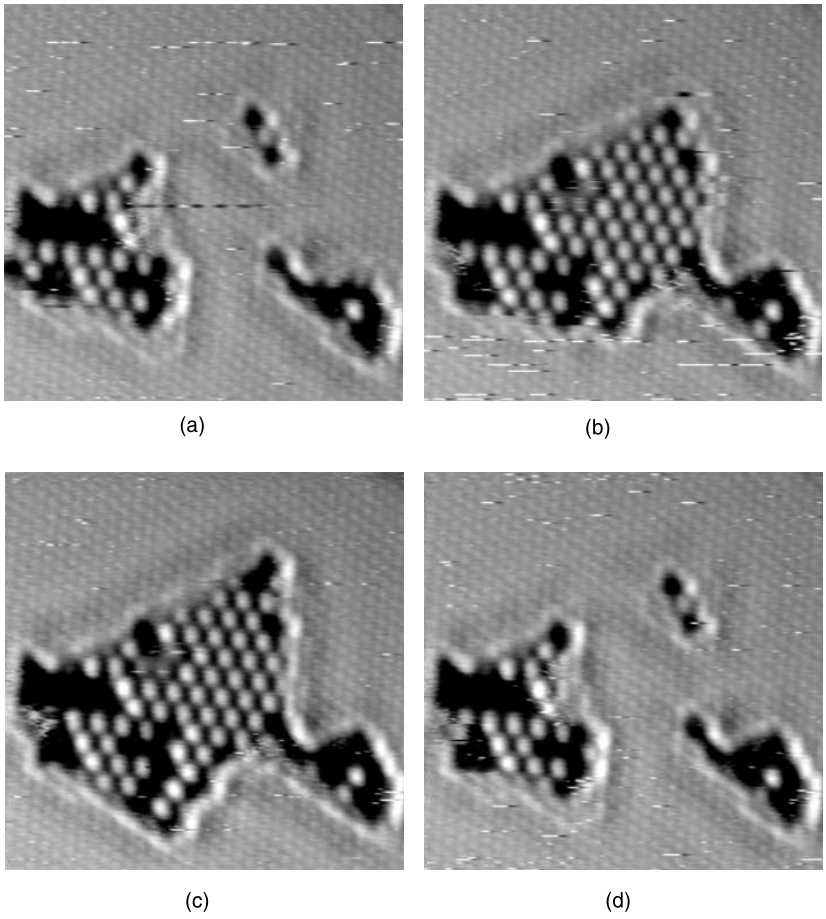

Fig. 2. Frames extracted from an STM movie showing fluctuations between a R3 island and the surrounding (1×1) region. The image size is 11×11 nm^2, and the tunneling conditions are $+0.15$ V and 0.1 nA. The starting time for each frame is (a) 0 s, (b) 64 s, (c) 96 s, (d) 192 s. The contrast in the images has been enhanced by merging the topography with its derivative in order to visualize the atomic resolution in both phases.

region was imaged first at $+1$ V (a), then at -1 V (b), back again at $+1$ V (c) and afterwards at -2 V (d). As it is clearly observed in this figure, the fluctuations are strongly influenced by the bias voltage. At negative sample voltages, the (1×1) region expands by diminishing the area of the R3 island seen in the middle of the figure. This reflects a tendency that was very often observed while scanning at relatively high voltages at negative sample polarity. At positive sample polarity a much slighter tendency in the opposite direction was observed.

In order to verify this point, other experiments were carried out where the STM tip was placed on R3 regions close to boundaries with the (1×1) and held statically without scanning (at typically 20–30 Å distance from the boundary) while the sample voltage was changed to higher absolute values (maintaining the feedback loop closed) during some seconds. Fig. 5 shows the result of one of those voltage pulses at negative sample bias. The region in the figure was first scanned at low bias ($+0.15$ V) (a), then a negative sample pulse of -3 V was applied for 25 s on the R3 spot marked with a cross and scanned again at low bias voltage (b). As deduced from the figure, the (1×1) region has expanded to the location where the voltage pulse was applied. In order to have reliable

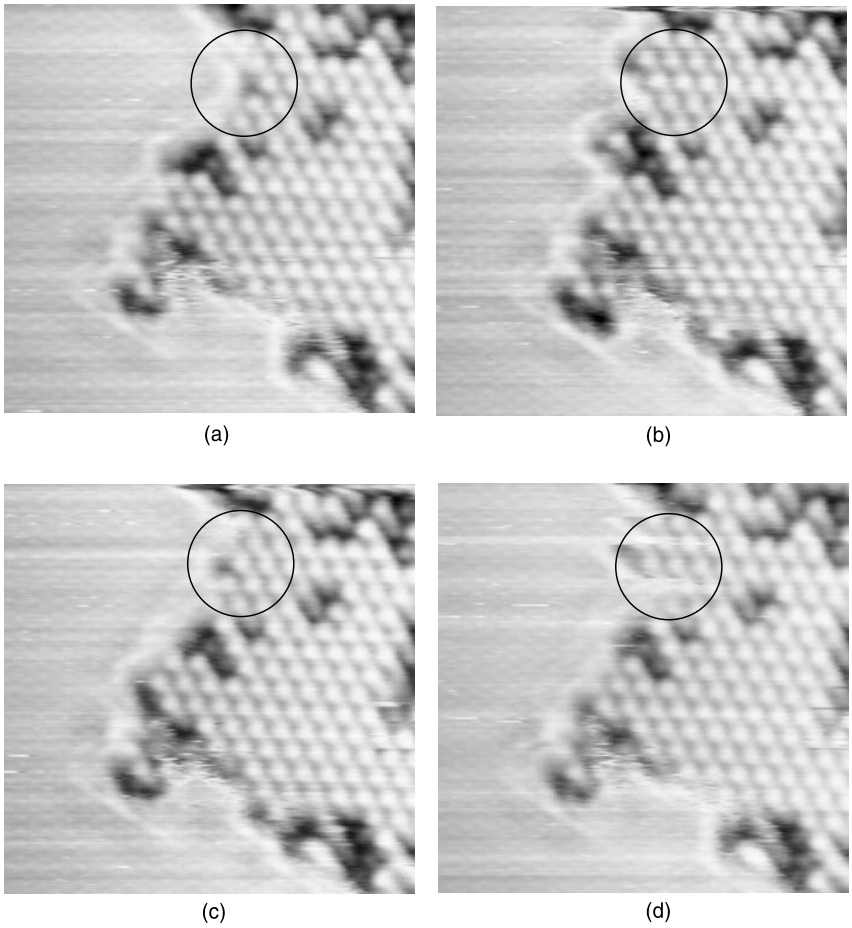

Fig. 3. Frames extracted from an STM movie measured on a boundary between (1×1) and R3 regions. The circles indicate the same spot in the surface (see main text). The starting time for each frame is: (a) 0 s, (b) 352 s, (c) 1376 s, (d) 1504 s. Image size: 11×11 nm^2. Tunneling conditions: $V = +0.15$ V, $I = 0.2$ nA.

statistics, more than a hundred pulses (of different voltage magnitude) were applied on different samples with different tips. Fig. 6 summarizes the results of these pulses at negative sample polarity. The percentage of successful pulses (i.e., leading to a R3 into (1×1) transformation) is displayed versus the magnitude of the pulse. For negative voltages lower in absolute value than a threshold that, although it was slightly tip dependent, lay around -1.5 V no significant influence was detected (at 20–30 Å distance from the boundaries). In contrast, for voltages in the range of -2 V to -4.5 V more than 50% of the pulses lead to induced transformations. For negative voltages higher in absolute value than -4.5 V, desorption processes from the surface started to be apparent. On the contrary, when positive sample voltages were applied, no significant STM induced variations on the boundaries were detected.

The transformation of a R3 into a (1×1) region implies that some extra Pb atoms are needed since the density of the (1×1) phase is higher than the atomic density in the R3. An important question to discuss is the origin of these atoms. One possibility could be that some Pb could come from some Pb hanging from the tip apex. A negative sample voltage pulse would induce the transfer of Pb atoms from the tip to the sample. This expla-

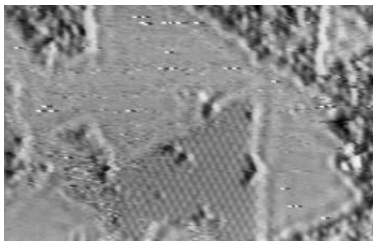

(a)

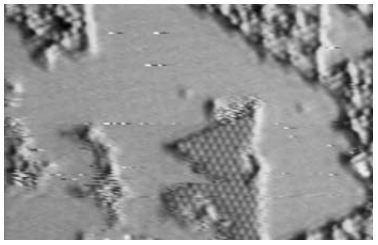

(b)

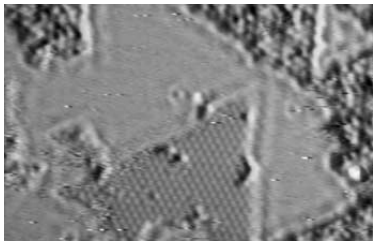

(c)

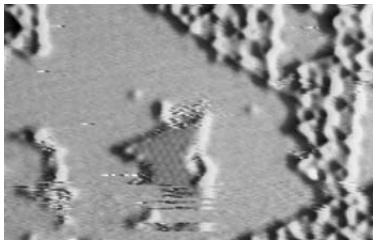

(d)

Fig. 4. 30×19 nm^2 STM images measured sequentially on the same area at different sample bias voltages ((a) +1 V, (b) −1 V, (c) +1 V, (d) −2 V). The tunnel current for all images is 0.1 nA. The contrast in the images has been enhanced by merging the topography with its derivative.

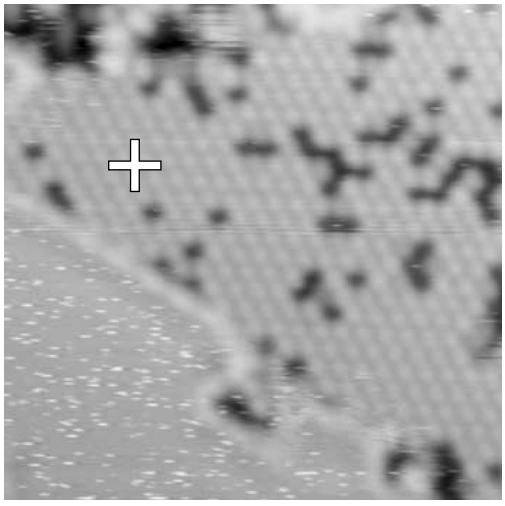

(a)

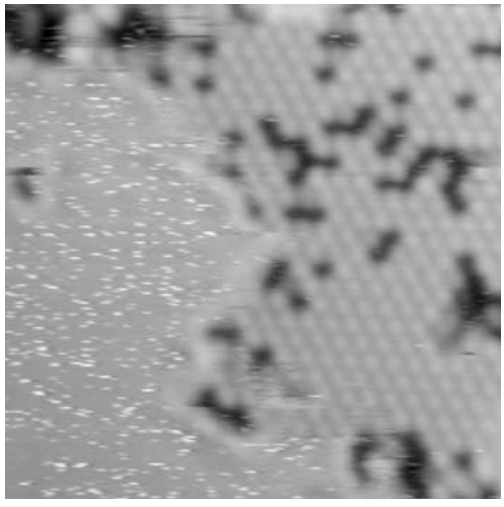

(b)

Fig. 5. STM images showing the effect of a −3 V sample voltage pulse of 25 s applied on the R3 spot marked by a cross in (a). The same area (15×15 nm^2) was scanned before (a) and after the pulse (b) at a sample voltage of +0.15 V and 0.2 nA.

nation, however, has to be rejected mainly based on two types of observations. On one hand, the detachment of atoms from the tip would in most cases imply a change in the STM resolution in subsequent imaging. As it is illustrated in Fig. 5 this is not the case in most of the voltage pulses in the range from −2 to −4.5 V. On the other hand, atom transfers between tip and sample can indeed be observed for voltage pulses higher in absolute value than ~4.5–5 V. At negative sample polarity, however, this high voltage pulses results in the detachment of Pb atoms from the surface and not

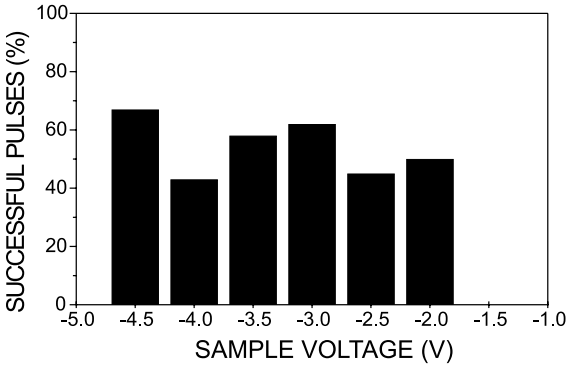

Fig. 6. Histogram showing the percentage of pulses applied on the R3 region leading to (1×1) transformation (successful pulses) versus the magnitude of the sample voltage pulse.

in R3 to 1×1 transformations. These observations rule out an explanation based on tip-sample atom transfer. This means that the extra Pb atoms must be the result of in-plane motion. In fact, it has been observed in the course of the present experiments that transformations of R3 regions into (1×1) as a consequence of a voltage pulse is accompanied by reciprocal transformations of (1×1) areas into R3 far away from the tip position.

All the results shown above suggest that the electrical field between the tip and the sample may certainly have an influence on the boundary fluctuations. STM field-induced surface diffusion was reported for the first time for Cs atoms on GaAs (1 1 0) surfaces by Whitman et al. [20] and has since then been reported for other adsorbates on semiconductor and metal substrates (see, for instance, Refs. [21–23]). This effect is explained [20] as the result of the modification of the effective potential energy distribution on the surface due to the presence of the inhomogeneous electric field (E) by an amount:

$$U_{\text{eff}}(\mathbf{r}) = -\boldsymbol{\mu}\mathbf{E}(\mathbf{r}) - \frac{1}{2}\boldsymbol{\alpha}\mathbf{E}(\mathbf{r})\mathbf{E}(\mathbf{r}) \quad (1)$$

where $\boldsymbol{\mu}$ is the static dipole moment and $\boldsymbol{\alpha}$ is the atom polarizability. The electric field potential energy gradient (in the radial direction under the tip) will result in a driving force:

$$\mathrm{d}U_{\text{eff}}/\mathrm{d}r \approx -(\mu + \alpha E)\mathrm{d}E/\mathrm{d}r \quad (2)$$

For the present experiments, the advancement of (1×1) regions towards the area under the tip when negative sample voltages are applied, while a much slighter effect and in the opposite sense when positive sample voltages are applied, could suggest that an effective static dipole moment exist in (1×1) regions. Thus, when negative sample voltages are applied, atoms from the high coverage (1×1) phase, which could be very mobile as mentioned above, would feel an effective driving force towards the area under the tip, increasing in that way the local coverage, and enhancing the probability to transform from the R3 to the (1×1) phase. At high positive sample voltages no driving force, or a very small one, would be present. In the context of such a simple model, a very rough estimate of the permanent atomic dipole moment necessary to compensate the induced dipole at positive voltages would yield an upper limit for the dipole moment of 0.2 e^- Å. [1] This is not in accord with the dipole charge of opposite sign and lower limit (0.05 e^- per surface atom) estimated from photoemission experiments on a different Si(1 1 1)(7 × 7)-Pb surface phase [6]. Nevertheless, charge transfer from Si adatoms to Pb adatoms in the R3 mosaic phase has been deduced from photoemission [8] and STM experiments [16].

The present data suggest that STM influence is not negligible at high negative bias voltages but cannot ascertain the intrinsic character of the fluctuations at low voltages. Further investigations are needed to clarify such complex behavior of the interface between (1×1) and R3 phases.

4. Conclusions

Complex dynamical processes take place at the interface between Pb/Si(1 1 1)-(1×1) and R3 phases. By means of STM we have been able to visualize fluctuations at the boundaries between domains of different reconstructed regions; these

[1] This order of magnitude rough estimation is based on an effective polarizability of the Pb atom, $\alpha \approx 7$ Å^3 [24] and a strength for the electric field of 0.5 V/Å, typical in STM experiments.

fluctuations have been resolved with atomic resolution for the first time. We have analyzed whether the fluctuations are intrinsic or STM induced and shown that at high bias voltages the STM electric field influence is not negligible. For high negative sample polarity Pb atoms from the (1×1) phase are driven towards the region under the tip when high voltages are applied, enhancing the probability to transform from the R3 to the (1×1) phase.

Acknowledgements

Very fruitful discussions with J. Gómez-Herrero, J.J. Sáenz and E. Artacho are kindly acknowledged. Financial support from DGES under contract number PB95-0169 is gratefully acknowledged.

References

[1] P.J. Estrup, J. Morrison, Surf. Sci. 2 (1964) 465.
[2] M. Saitoh, K. Oura, K. Asano, F. Shoji, T. Hanawa, Surf. Sci. 154 (1985) 394.
[3] G. Le Lay, J. Peretti, M. Hanbücken, W.S. Yang, Surf. Sci. 204 (1988) 57.
[4] E. Ganz, F. Xiong, I.-S. Hwang, J. Golovchenko, Phys. Rev. B 43 (1991) 7316.
[5] E. Ganz, I.-S. Hwang, F. Xiong, S.K. Theiss, J. Golovchenko, Surf. Sci. 257 (1991) 259.
[6] H.H. Weitering, A.R.H.F. Ettema, T. Hibma, Phys. Rev. B 45 (1992) 9126.
[7] J.A. Carlisle, T. Miller, T.-C. Chiang, Phys. Rev. B 45 (1992) 3400.
[8] C.J. Karlsson, E. Landemark, Y.-C. Chao, R.I.G. Uhrberg, Phys. Rev. B 45 (1992) 6321.
[9] L. Seehofer, D. Daboul, G. Falkenberg, R.L. Johnson, Surf. Sci. 307–309 (1994) 698.
[10] L. Seehofer, G. Falkenberg, D. Daboul, R.L. Johnson, Phys. Rev. B 51 (1995) 13503.
[11] I.-S. Hwang, R.E. Martinez, C. Liu, J.A. Golovchenko, Phys. Rev. B 51 (1995) 10193.
[12] J.M. Gómez-Rodríguez, J.J. Sáenz, A.M. Baró, J.-Y. Veuillen, R.C. Cinti, Phys. Rev. Lett. 76 (1996) 799.
[13] J.M. Gómez-Rodríguez, J.-Y. Veuillen, R.C. Cinti, Surf. Rev. Lett. 4 (1997) 335.
[14] J. Slézak, P. Mutombo, V. Cháb, Surf. Sci. 454–456 (2000) 584.
[15] Nanotec Electrónica S.L., http://www.nanotec.es.
[16] J.M. Gómez-Rodríguez, J.-Y. Veuillen, R.C. Cinti, Surf. Sci. 377–379 (1997) 45.
[17] J. Slezák, P. Mutombo, V. Cháb, Phys. Rev. B 60 (1999) 13328.
[18] A.J. Caamaño, Y. Pogorelov, O. Custance, J. Méndez, A.M. Baró, J.Y. Veuillen, J.M. Gómez-Rodríguez, J.J. Sáenz, Surf. Sci. 426 (1999) L420.
[19] X. Tong, K. Horikoshi, S. Hasegawa, Phys. Rev. B 60 (1999) 5653.
[20] L.J. Whitman, J.A. Stroscio, R.A. Dragoset, R.J. Celotta, Science 251 (1991) 1206.
[21] Y.W. Mo, Science 261 (1993) 886.
[22] A.A. Saranin, T. Numata, O. Kubo, H. Tani, M. Katayama, V.G. Lifshits, K. Oura, Phys. Rev. B 56 (1997) 7449.
[23] J. Méndez, J. Gómez-Herrero, J.I. Pascual, J.J. Sáenz, J.M. Soler, A.M. Baró, J. Vac. Sci. Technol. B 14 (1996) 1145.
[24] D.R. Linde (Ed.), Handbook of Chemistry and Physics, CRC Press, Boca Raton, 1990.